Characteristics of Energetic Ions Emitted from Hollow Cathodes*

Casey C. Farnell, John D. Williams, and Paul J. Wilbur
Department of Mechanical Engineering
Colorado State University
Fort Collins, CO 80523
Phone: (970) 491-8564
FAX: (970) 491-8671
e-mail: cfarnell@engr.colostate.edu

ABSTRACT

The behavior of a hollow cathode operated within an ion thruster discharge chamber is characterized using a remotely located, charged-particle analyzer. A very complex structure of the ion energy distribution function is revealed that is in general agreement with previous observations from many earlier works. Observations, which are in general agreement with the literature, include the measurement of ions that have "through anode" energies and beyond, that have higher ion energies occurring as flow rate is reduced, and that have higher discharge currents inducing more energetic ion production. All of these observations are also in line with results from long term life tests of hollow cathode-equipped ion thruster systems, which show erosion of hollow cathodes and components located nearby that is presumably caused by sputtering due to energetic ion bombardment. Most studies of hollow cathodes have concentrated on devices operated outside of discharge chambers where they are more readily accessible. This study is different in that it was performed with the hollow cathode located within a specially designed, 30-cm diameter discharge chamber. The measurements were made using a collimated electrostatic energy analyzer (ESA) that was sighted through a slot cut in the discharge chamber wall and pseudo grid surface. The hollow cathode/discharge chamber system could be rotated about an axis centered at the cathode orifice, and this enabled measurement of the ion energy distribution functions at zenith angles ranging from 0^o to 90^o with respect to the hollow cathode centerline. The ESA lateral position was also varied to look at regions located [in a line-of-sight (LOS) sense] on either side of the hollow cathode. Results are presented which show the effects of zenith angle variation, discharge current, and cathode flow rate on the ion energy distribution. Very interesting results obtained in recent experiments at high discharge currents are presented that show the ion energy distribution varying widely when measured at different zenith angles and at different positions near the hollow cathode. Specifically, few high-energy ions are seen on-axis, but many are seen at moderate (~20° and higher) zenith angles and from regions up to 5 cm from the cathode. This observation is different than those made on hollow cathodes operated outside of a discharge chamber.

INTRODUCTION

Hollow cathodes are utilized on plasma producing devices such as ion thrusters to supply electrons to the discharge plasma.[1] During extended life tests performed on NASA's NSTAR flight spare thruster, components at and near the hollow cathode have been observed to be completely eroded away presumably due to sputter erosion by energetic or multi-charged ion bombardment.[2] Although highly eroded, this thruster has now completed twice the on-mission life demonstrated by its flight twin. In an interesting twist, the very success of NASA's NSTAR flight thruster has opened the door to the consideration of much more ambitious missions for ion thrusters and their hollow cathode components. As spacecraft become larger and missions become more ambitious, it is necessary to increase the lifetimes of hollow cathodes and the components near them while simultaneously exposing them to progressively harsher operational conditions. The goal is to understand the mechanism by which energetic (possibly multi-charged)[3] ions are produced. The hope here is that once these mechanisms are understood they can be mitigated if not completely eliminated. An alternative would be to settle for the ability to specify the requirements of a sputter resistant component that could be placed near the cathode as a sacrificial remedy for a given discharge chamber operating condition.

Many studies have been performed where electron emission currents (in the form of arcs) are drawn from a surface or orifice into near vacuum conditions surrounding the emission site. Crofton and Boyd[3]

* Presented as paper IEPC-03-072 at the 28th Int'l Electric Propulsion Conf., Toulouse, France, 17-21 March 2003.

focus on measurements of low-flow hollow cathodes where they report both high-energy ions and significant numbers of multiply charged ions. Williams and Wilbur[4] performed studies on low-current, low-flow rate hollow cathodes where high-energy ions were measured and potential hill structures were detected. Friedly and Wilbur[5] and Kameyama and Wilbur[6] presented data on hollow cathodes operated at high currents (~50 A and higher) where very destructive high energy ions were detected. In work on a free arc pulled from a solid surface, Swift[7] discusses many instances where researchers have detected high-energy ions. Swift goes on to re-propose the potential hill or hump theory of high-energy ion production and then demonstrates its existence using evidence from retrograde motion studies in strong magnetic field environments. In a very high current regime of free arcs pulled from surfaces, Rusteburg et al.[8] present high energy ion data that display wide variations in zenith angle emission depending upon when the measurements are made during sinusoidal driven emission cycles. Davis and Miller[9] present exceptional data on energetic ions emitted from dc arcs where they also find significant numbers of multi-charged ions. It is noted especially that Compton[10] and also Tanberg[11] performed early studies that indirectly detected high-energy ion generation in vacuum arc environments. The studies discussed above date from the 1930s to the present and all discuss direct and inferred evidence of high-energy ions being generated within arcs. In addition, nearly all of the researchers listed struggle with explaining the mechanism responsible for accelerating the ions, and most suggest the potential hill (or hump) explanation.

The closest work to that presented here is that of Foster and Patterson[12] who used a fixed-position, highly collimated ESA to investigate the ion energy characteristics of ions flowing along the axis of an open-ended, 40-cm diameter ion thruster discharge chamber. Although they saw some evidence of high-energy ions, the energies are not excessive like they are in the present study under some operating conditions and some viewing locations. As will be pointed out below, very few high-energy ions flowing along the axis of the discharge chamber were observed in our study, which is in general agreement with Foster and Patterson. In this paper, we first describe the experimental setup used to measure the energy distribution of ions expanding from a discharge chamber plasma. In the following results section, the ion energy distribution is characterized as functions of the zenith angle at which the ions flow from the cathode region, propellant flow rate, and discharge current. Finally, conclusions and recommendations for future work are presented.

APPARATUS AND PROCEDURE

The experimental setup used is shown in Fig. 1. It consisted of a hollow cathode mounted within a rotatable discharge chamber and a remotely located electrostatic energy analyzer (ESA). The chamber had a 30-cm diameter cylindrical section attached to a conical central section which was capped by a back plate and was, therefore, similar in size, shape, and magnetic field geometry to the NSTAR thruster.[2] The discharge chamber was made from sheet aluminum with an inner stainless steel lining and three magnet rings as shown in Fig. 1. The three magnet (samarium cobalt) rings were mounted near the intersections of the back plate, conical, cylindrical and grid surfaces, and their poles were positioned to face axially, radially, and anti-axially, respectively. A pseudo-screen grid fabricated from stainless steel and biased to cathode potential was used to simulate the neutral flow restricting behavior of an actual ion optics system (e.g. the chamber was not operated in an open-ended fashion used by Foster and Patterson).[12] Ions produced in the plasma were allowed to flow directly from the discharge chamber through a 6-mm wide slot cut in the side wall of the discharge chamber and pseudo-screen grid so they could be sensed by the ESA. The discharge chamber/hollow cathode system was mounted within a fixture so that it could be rotated about an axis centered at the cathode orifice thereby enabling measurements at angles from 0^o to 90^o with respect to the cathode centerline. The setups in Fig. 1 show the chamber rotated to two positions for which the ESA is at angles of 90^o and 30^o with respect to the hollow cathode centerline (i.e. at zenith angles [θ] of 90^o and 30^o). The ESA was on a carriage that could be translated over the region suggested by the dashed lines in the figure. This enabled sighting of the ESA over a region that extended $x = \pm 50$ mm in a line-of-sight (LOS) fashion on either side of the cathode orifice. This was done to investigate the size and shape of the region of high-energy ion production suspected to be near the hollow cathode orifice.

The cathode/keeper assembly is shown in a side view and a view along the cathode axis looking down the orifice in Fig. 2. The hollow cathode was a 6.3 mm diameter tube that contained a low-work-function impregnated, sintered tungsten insert. The hollow cathode was equipped with an orifice plate that had a 0.55 mm diameter orifice on its centerline. The cathode insert was heated by a resistive coil wrapped around the outside of the hollow cathode tube that was insulated by a multiple-layer, tantalum-foil radiation shield. The enclosed keeper used with the cathode was equipped with an orifice plate fabricated from a 0.635 mm thick tantalum. The keeper orifice plate had a 2.54 mm diameter orifice positioned about 0.5 mm downstream of the cathode orifice plate. All of the xenon propellant required to operate the cathode and the

discharge chamber plasma were supplied through the cathode. Because high voltages were not applied to extract ions and propellant was lost only through the relatively small slot in the chamber side-wall and the pseudo-grid surface, this xenon flow rate was sufficient to produce nominal thruster operating conditions.

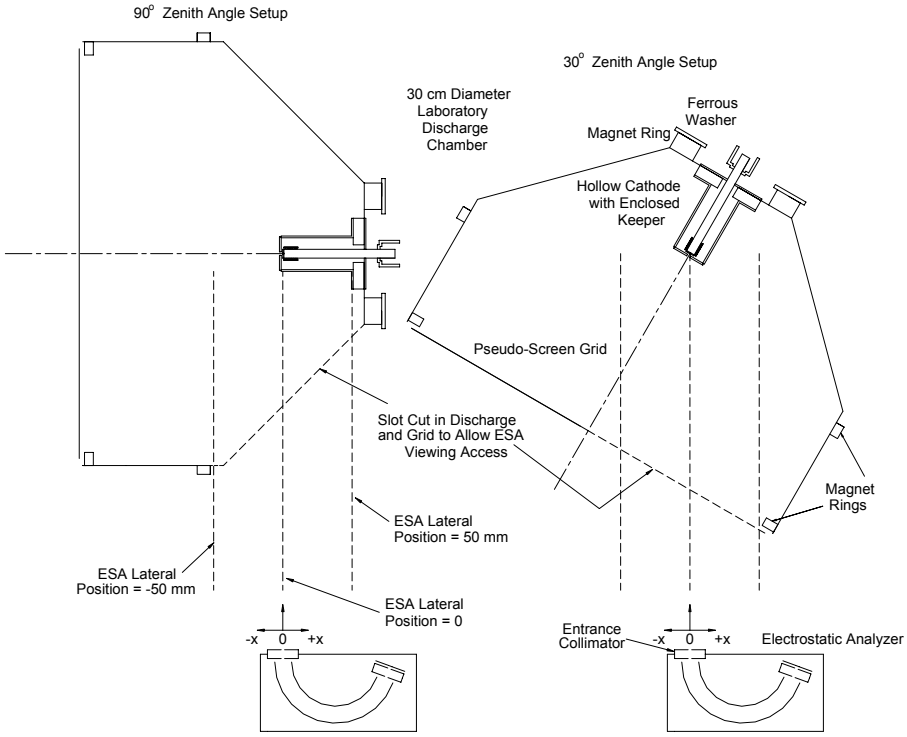

Fig. 1 Test apparatus showing ESA lateral sighting limits for 90° and 30° zenith angle setups.

Fig. 2 Cathode and keeper assembly with close-up view of keeper and cathode orifices.

The ESA was operated using a sector field sweep mode[13] to characterize ion energy. The ESA consisted of two spherical sector plates fabricated in a 160° arc. At each end of the arc, the ESA had a collimator to limit the field of view of the device. Both collimators were comprised of a set of two disks with 2 mm holes aligned with each other and separated by 1 cm to allow for very narrow solid angle acceptance of ions moving toward the detector. A nickel mesh was placed in front of the entrance aperture to shield the ESA from ambient plasma electrons that might penetrate the collimator assembly and flow around the spherical sectors to the collector electrode. The collector electrode was located downstream of the exit collimator and was well isolated from the plasma to ensure accurate current measurements. In order to collect all of the ions that passed through the ESA on the proper trajectories, a small negative DC bias was applied to the collector electrode to draw those ions to it. A computer was used to control a Keithley 617 programmable electrometer that applied both the desired potentials to the spherical plates through a resistive voltage divider circuit relative to the entrance and exit collimators and measured the ion current flowing to the collector. The voltage difference on the spherical plates was converted to ion energy using the equation:

$$E = \frac{\Delta V}{\frac{r_1}{r_2} - \frac{r_2}{r_1}}, \qquad \text{or for the ESA geometry used: } E = 2.254 * \Delta V$$

where r_1 and r_2 were the inner and outer radii of the ESA spherical segments and ΔV was the voltage difference applied between r_1 and r_2. Once the voltages were applied to the plates, a picoammeter built into the Keithley electrometer was used to measure the ion current that flowed to the collector electrode. It is noted that the transmission energy bandwidth varies during data collection when the ESA is operated in the sector field sweep mode due to the different bias conditions that are applied during the ion energy scan. This in turn causes a systematic perturbation in the collected ion current magnitudes. In particular, ion currents are perturbed in a nearly linear fashion to greater values as higher voltage differences are applied to the spherical sectors (e.g. the energy bandwidth increases with increasing voltage bias). One approximate method used to correct the data to obtain a true ion energy distribution function involves dividing by the bias voltage, which is about correct for high bias conditions. Because the correction required is relatively difficult to apply rigorously over the full bias voltage range commonly used, it is standard practice to present the data as is (i.e., without correction) and focus on the trends that are being observed instead. On this basis, the data presented in this paper have not been corrected for variable transmission energy bandwidth effects that are present when the sector field sweep mode of operation is used.

RESULTS AND DISCUSSION

Typical data obtained with the ESA sighted on the cathode from zenith angles over the range 0^o to 90^o when the thruster was operating at a nominal discharge current condition of 18 A are shown in Fig. 3. For this test, the ESA was sighted along a line pointed about 0.63 cm to the right of the cathode orifice. The heater current and voltage were 2.0 A and 2.94-2.97 V, the keeper current and voltage were 1.75 A and 10.3-10.5 V, and the discharge current and voltage were 18 A and 27.4-27.7 V at a flow rate of 3.9 sccm Xe. As can be seen in the figure, relatively large ion currents are sensed at energies near 30 eV for the 0^o and 10^o zenith-angle cases. The discharge voltage is near 30 V, and these signals are presumed to be due to discharge plasma ions. Because no ion current is observed above about 40 eV, it is argued that energetic ions are not ejected from the cathode region at these zenith angles. Going to higher zenith angles of 20^o to 90^o this condition changes, and high-energy ion signals are observed. The most probable energy of either the main discharge or high-energy ion signal is determined by looking at the energy where the maximum current was measured and the full-width, half-maximum (FWHM) energy spread is defined as the width of the signal at one half the current associated with the most probable energy. The high-energy ion signal reached a maximum at the 30^o zenith angle in both current magnitude (~ 80 pA) and most probable energy (~ 83 eV) for these operating conditions (FWHM = ~ 45 eV). The signal associated with main discharge ions was around 30 eV for the smaller zenith angles and dropped to ~25 eV for the 80^o and 90^o traces. Looking at the distribution taken at the 30^o zenith angle, it is noted that almost no signal associated with the main discharge ions was seen. This phenomenon will be looked at later when describing the effects of moving the ESA to positions other than those very near the cathode orifice. The trend shown, wherein there were no high-energy ion signals at the small zenith angles and there were substantial signals at the larger zenith angles, was observed at all operating conditions except those where no high-energy ion signal was measured at any zenith angle.

This result is substantially different than measurements made by Crofton and Boyd[3] and Wilbur and Kameyama[6] on freestanding hollow cathodes. Specifically, other studies differ from the above data in that they observed the greatest high-energy ion currents at zenith angles near 0^o when the ESA was pointed at the cathode orifice. It is believed that high-energy ions are not seen at low zenith angles in this study because the tests were conducted within a pseudo discharge chamber environment. As mentioned above, previous studies involved hollow cathodes that only used plates to collect the keeper and discharge current and no magnetic fields were applied. Therefore, it could be that effects associated with the magnetic field environment or other phenomena present in the discharge chamber were affecting the emission or focusing of high-energy ions from the hollow cathode. Another possibility is that the energetic ions were somehow being masked by the strong main discharge-plasma ion signal at low zenith angles while high-energy ions were seen at higher angles because the discharge plasma through which they passed to reach the ESA was less dense.

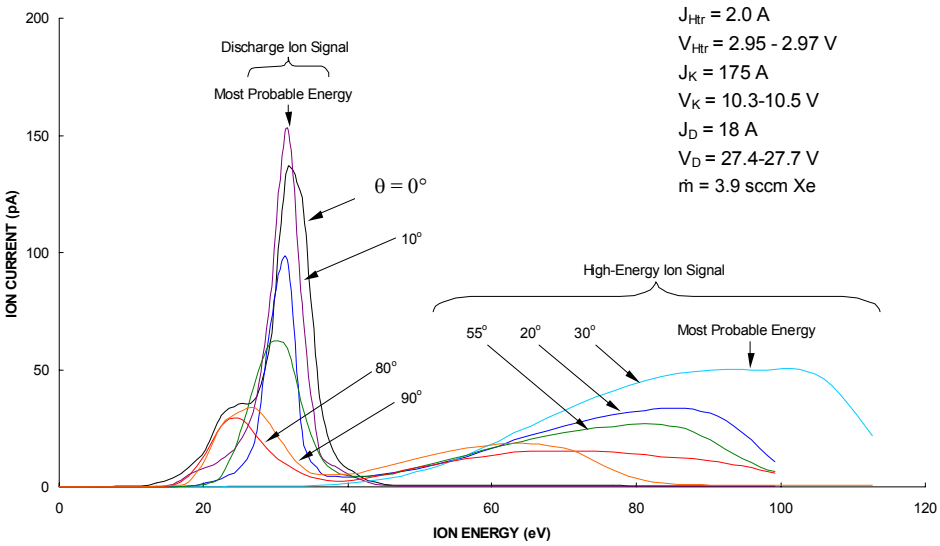

Fig. 3 Effect of zenith angle variation on the ion energy distribution with the ESA sighted along a line at x = +0.63 cm from the hollow cathode orifice (see Fig. 1).

As mentioned previously, a method was developed to enable lateral movement of the ESA with respect to the cathode orifice so regions both at and near the cathode orifice could be studied. Figure 4a-e shows contour plots of ion energy versus ESA lateral position at zenith angles of 0^o, 10^o, 30^o, 55^o, and 90^o when the discharge current and flow rate were 18 A and 3.9 sccm Xe, respectively. The contour levels on these plots have all been normalized using the magnitude of the greatest current signal observed during this test. Looking first at the 0^o zenith-angle case in Fig. 4a, it can be seen that a main discharge signal existed for all lateral ESA locations and that no high-energy ions were seen at any points near the cathode orifice. For the region from x = -25 to -50 mm, no data were taken because the line of sight (LOS) between the ESA collimator entrance and the discharge plasma was blocked by the pseudo-screen grid surface. For the 10^o zenith angle case in Fig. 4b, high main discharge ion signal currents were measured throughout the entire scanned region along with a small number of high-energy ions seen when the ESA was looking upstream of the cathode orifice at x = 50 mm. Figure 4c shows the plot associated with the 30^o zenith angle case. When the ESA was pointed downstream with respect to the cathode orifice from x = 0 to -50 mm, the main discharge signal had ion energies around 30 eV and high-energy ions (with a most probable energy near 60 eV) appeared when the ESA was sighted along a line downstream of the orifice at about x = 20 mm. In contrast, when the ESA was sighted upstream of the cathode orifice, from x = 0 to 50 mm, no discharge ion signal could be seen, but a high-current, broad, high-energy ion signal was observed that had energies varying from 50 to 100 eV (as indicated by the 0.05 contour line). A similar trend is followed in Fig. 4d at 55^o except the trend is less dramatic compared to the 30^o case and the current magnitudes are lower. There are no data presented outward of x = ± 25 mm because the line of sight between the ESA entrance and the plasma was obstructed by the discharge chamber structure that held the magnet rings in place. The main discharge signal was about 30 eV and was most prominent when looking along a line downstream of the cathode orifice from x = 0 to –20 mm, while the high-energy signal increased in most probable energy as the ESA was moved and sighted along a line upstream of the cathode from x = 0 to 20 mm. Finally, Fig. 4e shows ESA traces at a zenith angle of 90^o. In this case, small amounts of high-energy ions were recorded near and upstream of the cathode orifice that had energies from 30 to 45 eV. As the ESA was moved downstream of the cathode, out to x = -5.0 mm, the high-energy ion signal decreased and the main discharge ion signal increased in current magnitude. It was the case for most of the traces taken at zenith angles above 20^o that a main discharge signal was observed when looking downstream of the cathode. Furthermore at angles greater than 20° when the ESA was pointed at and upstream of the cathode orifice, the main discharge signal was observed to be smaller (or even non-existent) and a high-energy ion signal would frequently be observed. It was thought that there should be a main discharge signal recorded for all of the ESA positions because the plasma was present, based on visual observation, within the discharge chamber. This effect is seen most predominantly at the 30^o zenith angle and may be due to a product of the plasma being in the magnetic field environment and that not many of the main discharge ions coming from the chamber were at the correct incidence angle to be measured by the ESA. Another possibility is that the relationship between the potential on the pseudo grid, which was biased to cathode potential, was in some way affecting how the main discharge ions flowed from the chamber causing them to be detected improperly by the ESA.

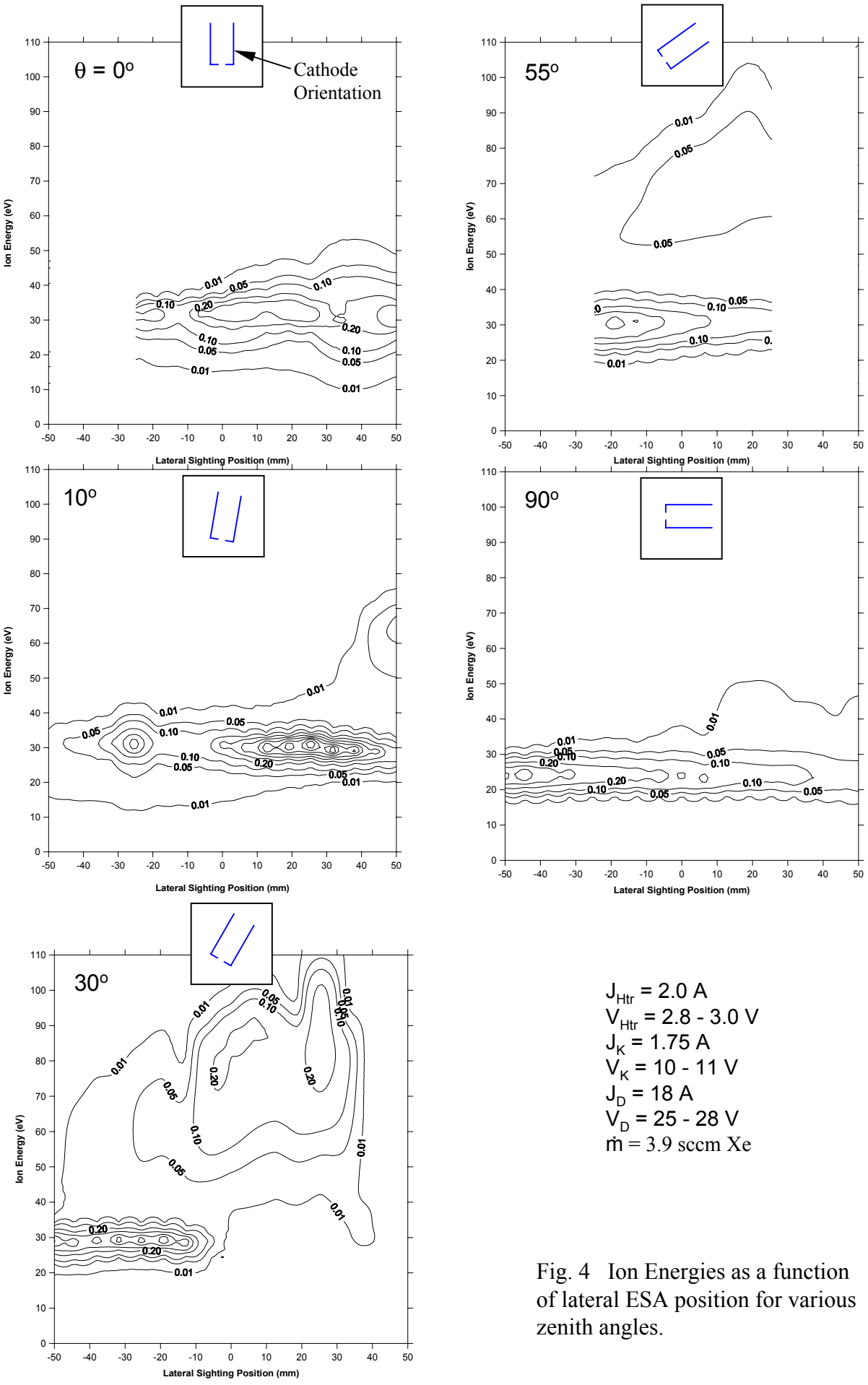

J_{Htr} = 2.0 A
V_{Htr} = 2.8 - 3.0 V
J_K = 1.75 A
V_K = 10 - 11 V
J_D = 18 A
V_D = 25 - 28 V
$\dot{m}$ = 3.9 sccm Xe

Fig. 4 Ion Energies as a function of lateral ESA position for various zenith angles.

Typical trends induced in the ion energy distribution function by changes in cathode flow rate and ESA sighting location are shown in Fig. 5 for the case where the zenith angle is 30°. Figure 5a shows three ion energy distribution function traces taken at a flow rate of 5.0 sccm Xe with the ESA sighted at the cathode orifice and at positions 1.27 cm on either side of the orifice. When the ESA was sighted at x = -1.27 cm and the ESA line of sight passed through the plume in front of the cathode (blue), both main discharge and high-energy ion signals were measured. On the other hand, when the ESA was sighted at x = +1.27 cm and did not pass through a cathode plume, no discharge ion signal was observed, but a strong high-energy signal was. The trace colored green, pointed at the cathode orifice, usually showed some evidence of discharge ions and a high-energy signal strength between those measured at positions displaced from the orifice. Figure 5b shows distributions measured at flow rates of 3.5, 3.9, 5.0, and 6.0 sccm Xe for the case when the ESA was sighted at x = +1.27 cm. Almost no main discharge signal was measured for any of these flow rates while a high-energy signal was seen in all cases. As the flow rate was decreased from 6.0 to 3.5 sccm Xe, the high-energy ion signal increased in both current magnitude and most probable energy. At the 3.5 sccm Xe level, the most probable energy of the high-energy signal was near 120 eV with a FWHM of about 47 eV. This trend is also seen in Fig. 5c for the case where the ESA was sighted at x = -1.27 cm. These distributions differ from those for x = +1.27 cm because they show a large discharge ion current signal along with the high-energy signal.

Figure 6 again shows the effects of varying cathode flow rate and ESA line of sight on the ion energy distribution function but in this case the zenith angle was set at 90°. Figure 6a shows three traces at a flow rate of 3.9 sccm Xe with the ESA sighted at the cathode orifice and at positions 1.27 cm on either side of the orifice. Both a main discharge ion signal and a high-energy ion signal were measured for all three of the ESA positions. Similar to Fig. 5, the main discharge ion signal was highest when the ESA was sighted (x = -1.27 cm) downstream of the cathode orifice and also the high-energy ion signal was the highest when the ESA was sighted (x = +1.27 cm) upstream of the cathode orifice. The trace colored green, which was sighted at the cathode orifice, showed ion signal strengths between the traces taken at positions off the cathode orifice. Figure 6b shows distributions measured at flow rates of 3.5, 3.9, 5.0, and 6.0 sccm Xe when the ESA was pointed upstream of the cathode orifice at x = +1.27 cm. For the 5.0 and 6.0 sccm Xe flow rates, no high-energy signal was seen, and only a small amount of current was recorded for the main discharge ion signal. As the flow rate was decreased to 3.9 and 3.5 sccm Xe, a high-energy ion signal was observed having energies from 40 to 70 eV along with a main discharge ion signal having energies from 20 to 30 eV. When the ESA was positioned at x = -1.27 cm as shown in Fig. 6c, the distributions followed a similar trend, as in Fig. 6b, with a broadening and increasing main discharge ion signal along with the development of a high-energy ion signal. As in the traces measured at 30°, the most probable energy of the high-energy ion signal increased as the flow rate was decreased. Comparing Fig. 5 with Fig. 6, the 30° case was observed to be much higher than the 90° case in both current magnitude and most probable energy for the four flow rates.

Discharge current was another operating parameter like cathode flow rate that affected the ion energy distribution function. Figure 7a shows the effect of varying discharge current on ion energy distributions measured at a zenith angle of 30° with respect to the cathode centerline. Examining the ion energy distributions colored blue, which were taken with the ESA sighted downstream of the cathode orifice at x = -1.27 cm, there was a main discharge signal having a most probable energy around 30 eV with no high-energy signal present for either the 10 or 14 A discharge currents. Conversely, the distributions colored orange were taken at x = +1.27 cm and no discharge ion signal was observed, but a high-energy ion signal was. In addition, the high-energy signal increased as the discharge current was increased. Similarly, Fig. 7b shows the effect of discharge current at a zenith angle of 90°. In this case, almost no high-energy ions were measured for either of the ESA positions. However, there was a small group of ions in the tail of the main discharge signal that were measured at x = +1.27 cm upstream of the cathode orifice.

It is mentioned that many other operational conditions were investigated during this study. In particular, several investigations were performed at low discharge currents (e.g. from 0 to 3 A) under different flow rate and keeper current conditions. In some instances at high keeper current and relatively low flow rate (at discharge currents of 0 A), high-energy ions have been observed at a 0° zenith angle. However, as soon as a discharge current was initiated (as low as 0.5 A) this feature would disappear and be replaced by a typical lower energy, discharge ion signal.

CONCLUSIONS AND RECOMMENDATIONS FOR FUTURE WORK

An initial study has been completed that looked at effects of zenith angle variation, propellant flow rate, and discharge current on the production of high-energy ions emitted from a hollow cathode that was

Fig. 5a x = 0, -1.27, +1.27 cm
ṁ= 5.0 sccm Xe

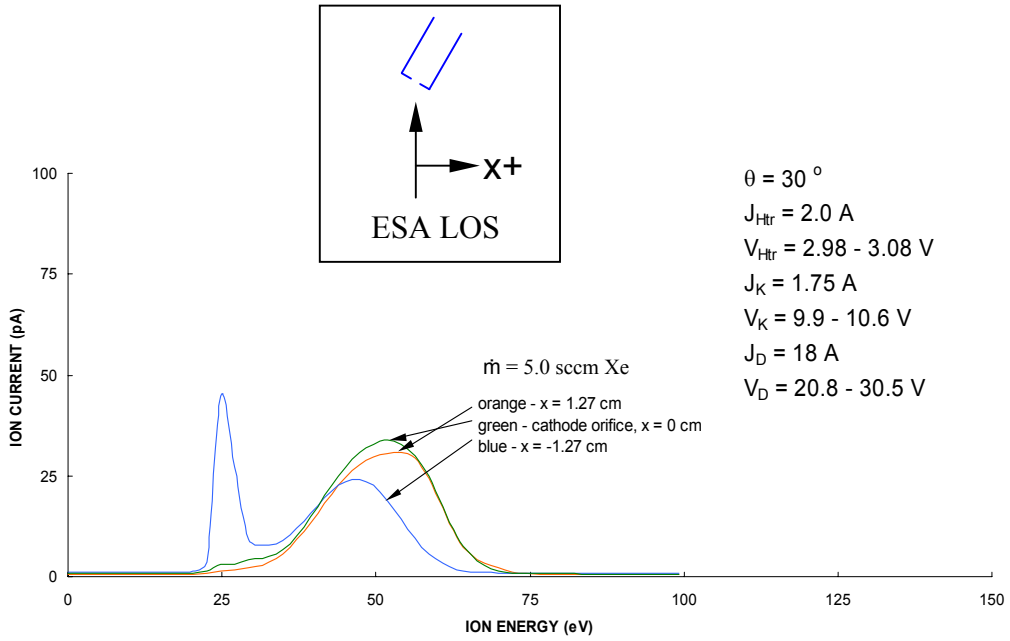

Fig. 5b
x = +1.27 cm

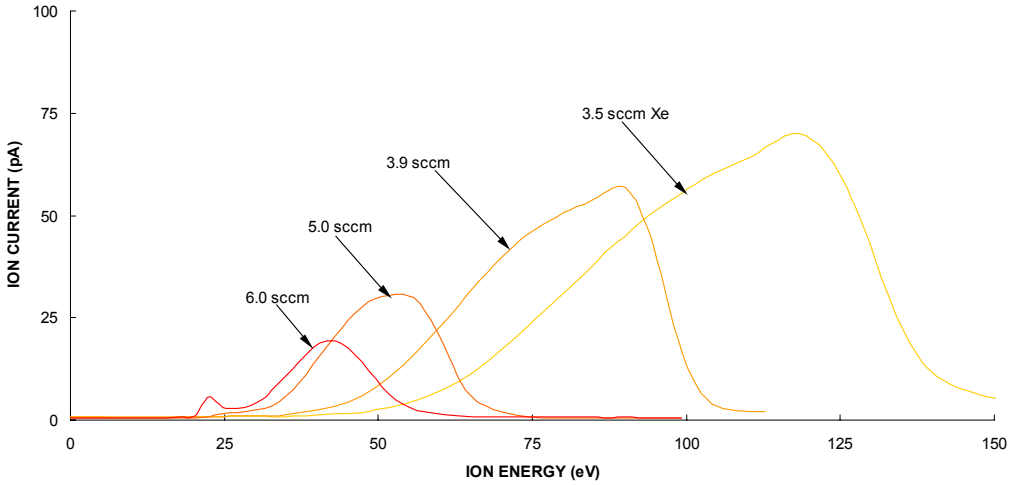

Fig. 5c
x = -1.27 cm

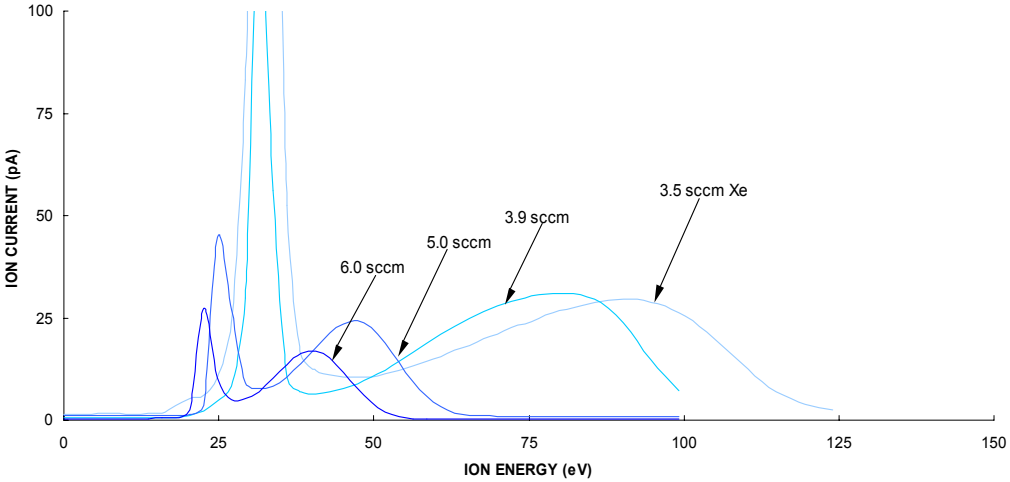

Fig. 5 Effect of flow rate on ion energy distributions measured at a zenith angle of 30° with the ESA sighted at hollow cathode regions located at x = 0 and x = ±1.27 cm.

Fig. 6a x = 0, -1.27, +1.27 cm
$\dot{m}$ = 3.9 sccm Xe

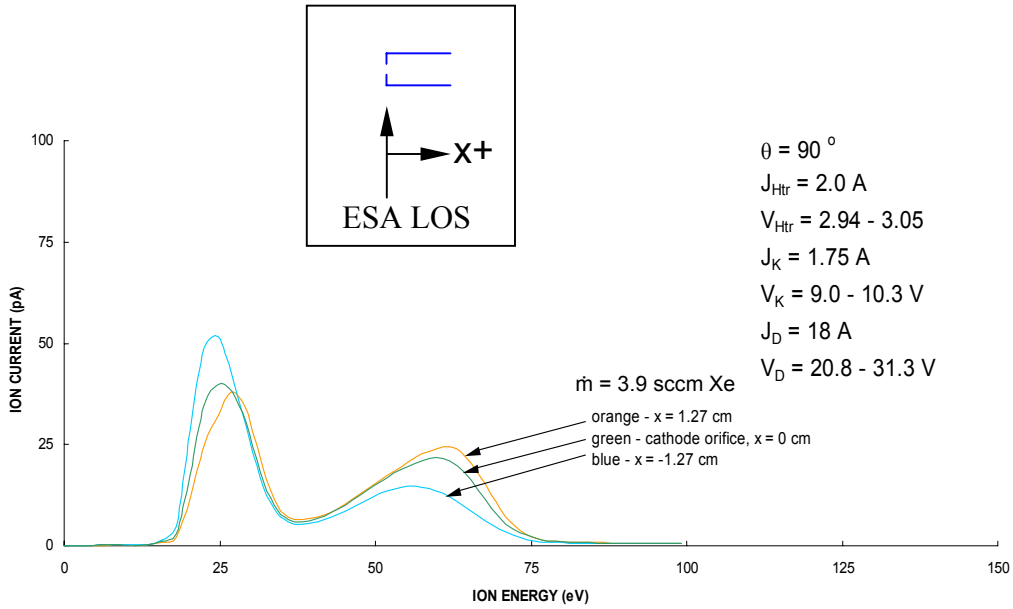

Fig. 6b
x = +1.27 cm

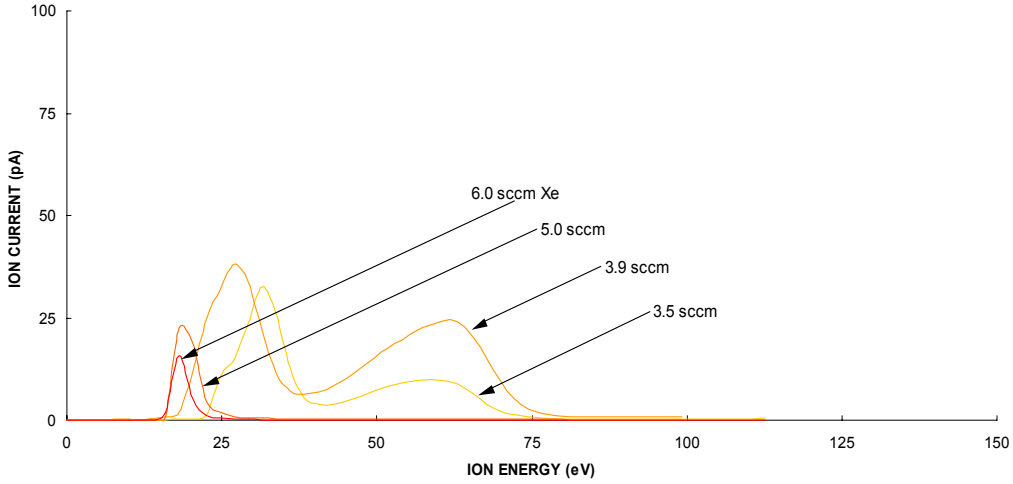

Fig. 6c
x = -1.27 cm

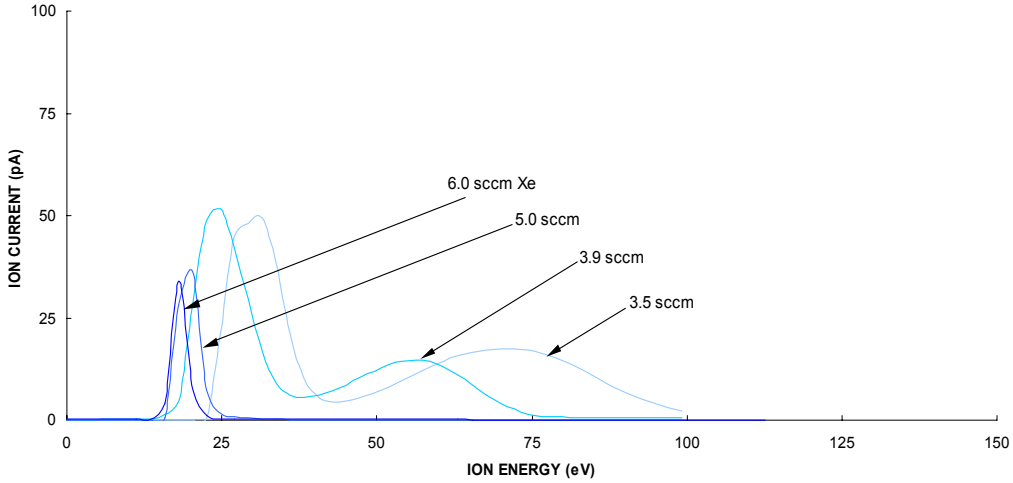

Fig. 6 Effect of flow rate on ion energy distributions measured at a zenith angle of 90° with the ESA sighted at hollow cathode regions located at x = 0 and x = ± 1.27 cm.

Fig. 7a Zenith angle = 30°

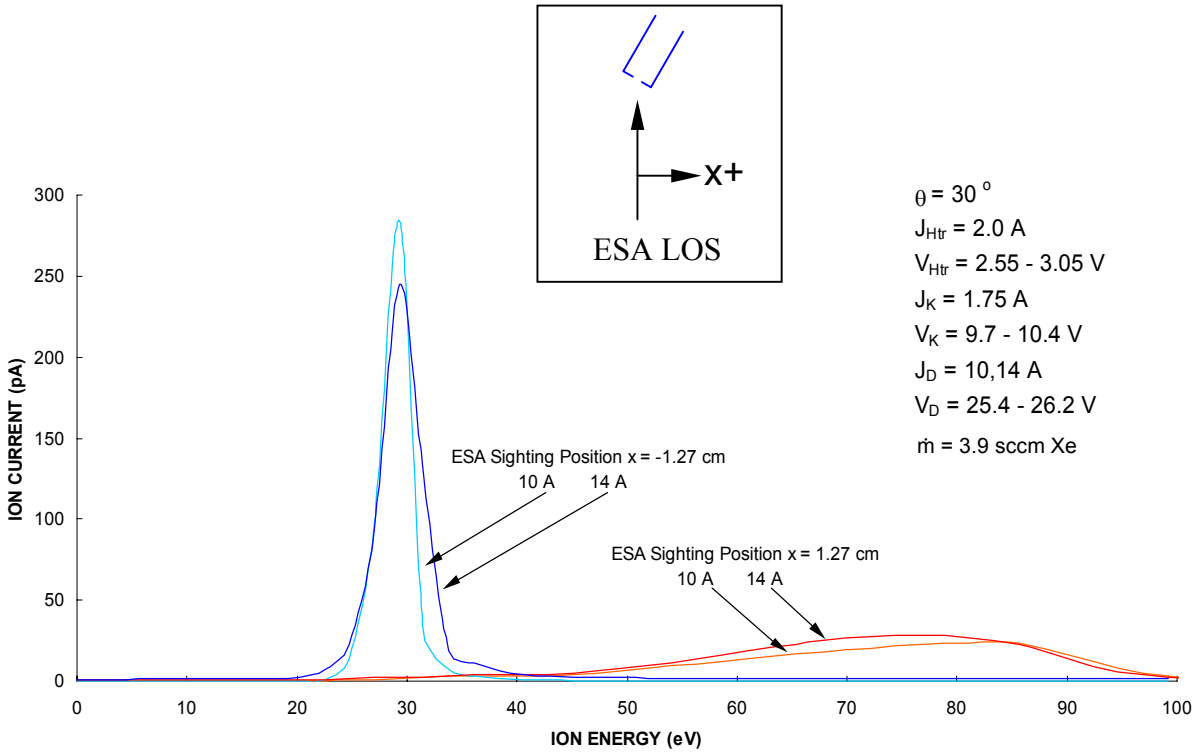

Fig. 7b Zenith angle = 90°

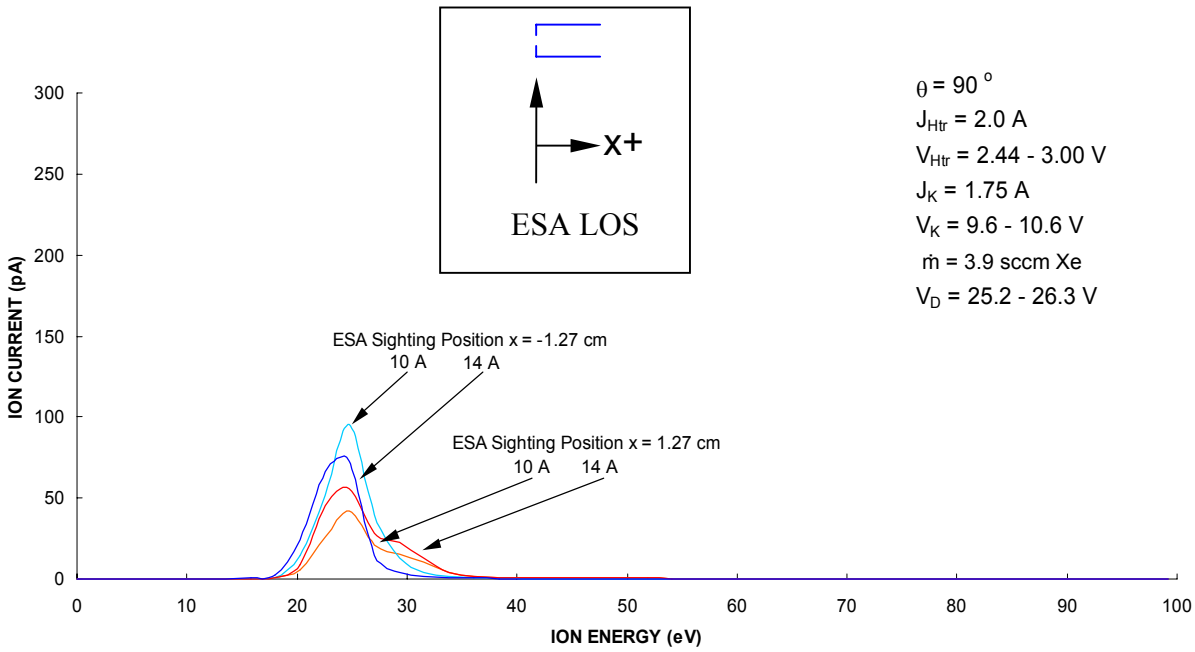

Fig. 7 Effect of discharge current variation on the ion energy distribution at zenith angles of 30° and 90°.

operated within a simulated discharge chamber environment. Using an ESA to measure ion energy distributions, the results showed a wide variation of high-energy ion production when the ESA was positioned at different zenith angles with respect to the cathode centerline. In particular, no high-energy ions were measured along the cathode centerline at high discharge currents, which is in conflict with observations made in previous studies on freestanding hollow cathodes. It was shown that a wide range of ion energies were measured depending on where the ESA was sighted with respect to the cathode orifice, especially at a zenith angle of 30^{o}. Experimental trends uncovered include (1) as flow rate was decreased ion energies increased and (2) as discharge current was increased ion energies increased. These two observations are in agreement with previous studies of freestanding hollow cathode experiments. In addition, it is pointed out that, in congruence with other researchers, there is a link between hollow cathode arc phenomena and general arc phenomena that has been studied for many years. The link is that ion energy ions are observed whenever high electron currents are drawn (in the form of an arc) from small regions where not quite enough flow rate or evaporation rate exists either do to choice (orificed hollow cathodes) or do to chosen material properties (conventional arc devices). In terms of future work, it is believed that ion energy measurements made with the remotely located ESA described herein can be used to construct the potential variation within the discharge chamber in the volume surrounding the hollow cathode device. Once this is accomplished, comparisons could be made to predictions of this structure obtained from existing (or future to be developed) numerical codes. Also important are energy distribution measurements of multiply charged ions that could be performed using advanced ESAs equipped with time-of-flight apparatus for exampole. In terms of indirectly measuring the existence of high-energy ions, erosion sensitive witness plates could be positioned within simulated discharge chambers to document the erosive characteristics of the discharge plasma on various surfaces.

ACKNOWLEDGEMENTS

This work was supported by a research grant from the Jet Propulsion Laboratory under contract 1232407.

REFERENCES

[1] Fearn, D.G., and C.M. Philip, "An Investigation of Physical Processes in a Hollow Cathode Discharge," AIAA Journal, Vol. 11, 1973, pp. 131-132. See also D.E. Siegfried and P.J. Wilbur, "A Phenomenological Model Describing Orificed, Hollow Cathode Operation," 15th International Electric Propulsion Conference, AIAA 81-0746, 1981. D.E. Siegfried and P.J. Wilbur, "A model for Mercury Orificed Hollow Cathodes: Theory and Experiment," AIAA Journal, Vol. 22, 1984, pp. 1405-1412.

[2] Sengupta, A., J.R. Anderson, J.R. Brophy, V.K. Rawlin, and J.S. Sovey, "Performance Characteristics of the Deep Space One Ion Thruster Long Duration Test after 21,300 Hours of Operation," 38th Joint Propulsion Conference, AIAA 2002-3959, 2002.

[3] M.W. Crofton and I.D. Boyd, "Plume Measurement and Modeling Results for a Xenon Hollow Cathode," 38th Joint Propulsion Conference, AIAA-2002-4103, 2002.

[4] J.D. Williams and P.J. Wilbur, "Electron Emission from a Hollow Cathode-Based Plasma Contactor," J. of Spacecraft and Rockets, Vol. 29, No. 6, November-December, 1992, pp.820-829.

[5] Friedly, V.J., and P.J. Wilbur, "High Current Hollow Cathode Phenomena," J. Propulsion and Power, Vol. 8, No. 3, 1992, pp. 635-643.

[6] Kameyama, I., and P.J. Wilbur, "Measurement of Ions from High-Current Hollow Cathodes Using Electrostatic Energy Analyzers," J. of Propulsion and Power, Vol. 16, No. 3, 2000, pp. 529-535.

[7] Swift, P.D., "Cathode- and Anode-Spot Tracks in a Closed Magnetic Field,"J. Appl. Phys., V.67, N.4, 1990, pp. 1720-1724.

[8] Rusteberg, C., M. Lindmayer, B. Juttner, and H. Pursch, "On the Ion Energy Distribution of High Current Arcs in Vacuum," IEEE Trans. on Plasma Science, Vol. 23, No. 6, 1995, pp. 909-914.

[9] Davis, W.D., and H.C. Miller, "Analysis of the Electrode Products Emitted by DC Arcs in a Vacuum Ambient," J. Appl. Phys., Vol. 40, No. 5, 1969, pp. 2212-2221.

[10] Compton, K.T., "On the Theory of the Mercury Arc," Physical Review, Vol. 37, 1931, pp. 1077-1090.

[11] Tanberg, R., "On the Cathode of an Arc Drawn in Vacuum," Physical Review, Vol. 35, 1930, pp. 1080-1089.

[12] Foster, J.E., and M.J. Patterson, "Plasma Emission Characteristics from a High Current Hollow Cathode in an Ion Thruster," 38th Joint Propulsion Conference, AIAA-2002-4102, 2002.

[13] Comstock, Inc. Double Focusing Electrostatic Energy Analyzer, User's Manual model AC-901, Oak Ridge, TN 37830. See also M.E. Rudd in Low Energy Electron Spectrometry, edited by K.D. Sevier, John Wiley & Sons, New York, 1972.